Theor Chem Acc (2010) 125:471–479
DOI 10.1007/s00214-009-0653-6

REGULAR ARTICLE

A wavelet-based adaptive method for determining eigenstates of electronic systems

Szilvia Nagy · János Pipek

Received: 31 March 2009 / Accepted: 18 September 2009 / Published online: 27 October 2009

Abstract The possibilities for reducing the necessary computation power in wavelet-based electronic structure calculations are studied. The expansion of the expectation values of energy operators, the integrals of basis functions are mostly system-independent, consequently it is not necessary to compute them in each calculations. Fixed building blocks, such as a parameterized expansion of the nuclear and electron–electron cusp can reduce the amount of necessary calculation. An algorithm for local expansion refinement is also given. It is possible to determine the significant expansion coefficients of a high resolution level without solving the Schrödinger equation using only lower resolution results.

Keywords Wavelet · Local refinement · Resolution level · Nuclear and electron–electron cusp · Adaptive algorithm

1 Introduction

Although wavelet analysis is not an old tool in mathematics, its practical importance is already proven, e.g., by the image and motion picture compressing algorithms based on wavelets [1–4]. Since this particular approach can be rather flexibly applied to solving problems, multiresolution analysis (MRA) or wavelet analysis is widely used in various fields of science, also in molecular and solid state physics. Simple quantum mechanical test systems were studied using finite level MRA approximations [5, 6], local density approximation calculations were carried out using wavelet basis sets [7], and even more sophisticated methods, like the evaluation of Kohn–Sham equations were modified to wavelet basis [8, 9]. Most of the methods are tested in one dimension, however, benchmark calculations for the quasi 2D homogeneous electron gas using wavelets demonstrated the computational feasibility of the approach [10]. A multiresolution algorithm in three dimensions has been suggested for calculating the Hartree–Fock exchange operator and for a solution of the local density approximation of the Kohn–Sham equation [11, 12]. Interesting mathematical extensions of treating the one-particle Schrödinger equation in curvilinear coordinates with wavelets have been published, as well [13, 14].

In MRA applications the rapid changes, which need high resolution for sufficiently precise description, are localized to certain intervals of the studied function. Wavelet analysis is able to change the resolution locally and this property is useful also in quantum mechanics. Quick changes of the wave functions and density matrices are usually concentrated to specific regions, like the surrounding of an atomic core. The distant fields of a molecule can be described at a rather rough resolution level with a grid distance of 0.5–0.25 atomic units and the extension of regions where further refinement is necessary near nuclear cusps shrinks exponentially as the resolution increases [15].

Dedicated to Professor Sandor Suhai on the occasion of his 65th birthday and published as part of the Suhai Festschrift Issue.

S. Nagy
Department of Telecommunication, Jedlik Ányos Institute of Informatics, Electrical and Mechanical Engineering, Széchenyi István University, Egyetem tér 1, 9026 Gyor, Hungary

J. Pipek (✉)
Department of Theoretical Physics, Institute of Physics, Budapest University of Technology and Economics, 1521 Budapest, Hungary
e-mail: pipek@phy.bme.hu

In the following review-like contribution, we summarize several aspects of our previous developments on the wavelet expansion possibilities of density matrices and related quantities, like expectation values of energy operators. Besides a general overview, the emphasis is put on the resolution of a serious problem encountered during the practical applications. Namely, the price to be paid for an overall better description is extremely high, as the number of basis functions increases exponentially with increasing resolution level. Consequently, an especially careful selection process of the extension of the basis set is of paramount importance. Critical areas in this respect are the surroundings of nuclear and electron cusps. A possibility to include the Kato electron–electron cusp condition [16] in the calculations is discussed. An illustration of the MRA description of nuclear and electron–electron cusps is presented for the three dimensional He atom. A method for an a priori determination of the highly detailed regions of wave functions based on the already calculated lower resolution level expansion coefficients is also given, and compared with other methods. This *adaptive* refinement algorithm is tested by numerical comparisons to analytical solutions of one dimensional systems.

2 Wavelets and scaling functions: the concept of MRA

Multiresolution analysis of the square integrable functions' Hilbert space $L^2(\mathbb{R})$ is a sequence of its closed subspaces $\{V_m,\ m \in \mathbb{Z}\}$ which are embedded into each other. The basis functions of V_m (the scaling functions) are shifted versions of a given function s_{m0} on an equidistant grid. As the resolution level m increases, both the scaling functions and the grid distance b are compressed by a given factor a. Thus the (orthonormal) basis of subspace V_m is the set of functions $\{s_{m\ell}(x)|\ell \in \mathbb{Z}\}$, where $s_{m\ell}(x) = a^{m/2}s_0(a^m x - b\ell)$. The values $a = 2$ and $b = 1$ are commonly used and the function $s_0(x)$ is usually referred as the mother scaling function.

The basis functions of a resolution level m can be expanded by the scaling functions of the finer level $m + 1$, using the *refinement equation*

$$s_{m\ell}(x) = \sum_{k=0}^{N_s} p_k s_{m+1k+2\ell}(x), \tag{1}$$

with $\sum_{k=0}^{N_s} p_k = 2$. If only a finite number N_s of non-zero expansion coefficients p_k are chosen, the mother scaling function s_0 has finite support, namely, s_0 is zero outside of the interval $[0, N_s)$ [17, 18].

An mth level approximation of the function $f \in L^2(\mathbb{R})$ arises as

$$P_m f(x) = f^{[m]}(x) = \sum_{\ell} c_{m\ell} s_{m\ell}(x), \tag{2}$$

with $c_{m\ell} = \langle s_{m\ell}|f\rangle$. Here, P_m is the projector to the subspace V_m.

Let the *detail space* W_m be the orthogonal complement of V_m in the finer subspace V_{m+1}

$$V_{m+1} = V_m \oplus W_m. \tag{3}$$

In W_m a basis set can be defined as $w_{m\ell}(x) = 2^{m/2}w_0(2^m x - \ell)$ generated from the mother wavelet w_0 by dilations and shifting, similarly to the scaling functions. The elements of the basis set $\{w_{m\ell}(x)|\ell \in \mathbb{Z}, m = 0, 1, \ldots\}$, i.e., the *wavelets*, are also compactly supported, if the scaling functions are of that kind. They can be expanded as

$$w_{m\ell}(x) = \sum_{k=1-N_s}^{1} q_k s_{m+12\ell-k}(x) \tag{4}$$

with $q_k = (-1)^k\, p^*_{-k+1}$.

Starting with resolution level m_0, an Mth level expansion ($M > m_0$), is a projection to the subspace

$$V_M = \bigoplus_{m=m_0}^{M-1} W_m \oplus V_{m_0}. \tag{5}$$

The approximation $P_M f$ can be equivalently expanded as

$$f^{[M]}(x) = \sum_k c_{Mk} s_{Mk}(x) \tag{6}$$

$$f^{[M]}(x) = \sum_k c_{m_0k} s_{m_0k}(x) + \sum_{m=m_0}^{M-1} \sum_k d_{mk} w_{mk}(x). \tag{7}$$

Supposing that the function f is enclosed in a box by restricting the summations for a finite set of k, the number of coefficients $\{c_{Mk}\}$ in expansion (6) equals to the total number of coefficients $\{c_{m_0k}, d_{mk}\}$ $\{c_{m0k},\ d_{mk}\}$ in (7), independent of the starting level m_0, and scales as $\sim 2^{DM}$ in D dimensions. However, it is not necessary to keep all the expansion coefficients d_{mk}, if in a region a lower resolution level is sufficient. Using wavelets and ignoring the sufficiently small coefficients of type d_{mk} can lead to a manageable number of necessary basis functions even in case of molecules, as we have shown in [15].

3 Calculating the integrals of scaling functions

In overlap and kinetic energy matrix element calculations integration of products of scaling functions and its derivatives satisfying the refinement equation

$$\varphi_j(x) = 2^{1/2} \sum_{\ell \in \mathbb{Z}} \bar{p}_\ell^{(j)} \varphi_j(2x - \ell) \tag{8}$$

is necessary. Consecutive applications of the integral variable transformation $x \to 2^{-m}x$ and substitutions of the refinement equation (8) lead to the calculation of the symbols

$$H(\alpha_1,\ldots,\alpha_n)=\int \varphi_0(x)\prod_{j=1}^{n}\varphi_j(x-\alpha_j)\mathrm{d}x. \tag{9}$$

The values of $H(\alpha_1, \ldots, \alpha_n)$ can be calculated by solving the eigenvalue equation

$$H(\alpha_1,\ldots,\alpha_n)=\sum_{\mu_1,\ldots,\mu_n\in\mathbb{Z}} h_{2\alpha_1-\mu_1,\ldots,2\alpha_n-\mu_n}H(\mu_1,\ldots,\mu_n) \tag{10}$$

with $h_{\vec{\mu}}$ arising from the coefficients in the refinement equations

$$h_{\vec{\mu}}=h_{\mu_1,\ldots,\mu_n}=\sum_{\gamma\in\mathbb{Z}} p_{\gamma}^{(0)}\prod_{j=1}^{n}p_{\gamma-\mu_j}^{(j)}. \tag{11}$$

A more detailed discussion of the above procedure can be found in [19]. An efficient algorithm for calculating more specific integrals appearing in DFT calculations is applied in the ABINIT software package and published in [20].

4 MRA expansion of density matrices

For spin variables, we have introduced scaling function spinors as the one-electron basis set [22] according to

$$s_{\mathbf{m}}(\mathbf{x})=s_{m\ell s}(\mathbf{r},\sigma)=s_{m\ell}(\mathbf{r})\delta_{s\sigma} \tag{12}$$

with $\mathbf{m}=(m,\ell,s)$. Later, Flad et al. [21] have also analyzed the structure of wavelet representations of correlated wave functions. In the following considerations expansion (6) is applied for the mth order approximation of the wave function. The N-electron basis functions are built as

$$\chi_\mu(\mathbf{x}_1,\ldots,\mathbf{x}_N)=(N!)^{-1/2}\begin{vmatrix} s_{\mathbf{m}_1}(\mathbf{x}_1) & \ldots & s_{\mathbf{m}_1}(\mathbf{x}_N)\\ \vdots & \ddots & \vdots\\ s_{\mathbf{m}_N}(\mathbf{x}_1) & \ldots & s_{\mathbf{m}_N}(\mathbf{x}_N)\end{vmatrix}, \tag{13}$$

where multiindex μ denotes the set of indices $\mu=(\mathbf{m}_1,\ldots,\mathbf{m}_N)$. A general N-particle wave function Ψ can be written as

$$\Psi(\mathbf{x}_1,\ldots,\mathbf{x}_N)=\sum_{\mu} c_\mu\chi_\mu(\mathbf{x}_1,\ldots,\mathbf{x}_N) \tag{14}$$

with complex coefficients $c_\mu=\alpha_\mu+i\beta_\mu$, where α_μ and β_μ are real. Using the scaling function decomposition (14), the pure state N-particle density matrix

$$\gamma_N(\mathbf{x}_1,\ldots,\mathbf{x}_N|\mathbf{x}'_1,\ldots,\mathbf{x}'_N)=\Psi(\mathbf{x}_1,\ldots,\mathbf{x}_N)\Psi^*(\mathbf{x}'_1,\ldots,\mathbf{x}'_N) \tag{15}$$

leads after partial trace operations to the spin-traced two-particle density matrix of the form

$$\gamma_2^{s[m]}(\mathbf{r}_1,\mathbf{r}_2|\mathbf{r}'_1,\mathbf{r}'_2)=\sum_{\substack{k_1,k_2\\ \ell_1,\ell_2}}\Big[g^{A,m}_{k_1k_2\ell_1\ell_2}\vartheta^{A,m}_{k_1k_2\ell_1\ell_2}(\mathbf{r}_1,\mathbf{r}_2|\mathbf{r}'_1,\mathbf{r}'_2) +g^{B,m}_{k_1k_2\ell_1\ell_2}\vartheta^{B,m}_{k_1k_2\ell_1\ell_2}(\mathbf{r}_1,\mathbf{r}_2|\mathbf{r}'_1,\mathbf{r}'_2)\Big] \tag{16}$$

where coefficients $g^{A,B,m}_{k_1k_2\ell_1\ell_2}$ are real numbers. The functions

$$\begin{aligned}\vartheta^{A,m}_{k_1k_2\ell_1\ell_2}(\mathbf{r}_1,\mathbf{r}_2|\mathbf{r}'_1,\mathbf{r}'_2)=\frac{1}{2}\Big[&s_{mk_1}(\mathbf{r}_1)s_{mk_2}(\mathbf{r}_2)s^*_{m\ell_1}(\mathbf{r}'_1)s^*_{m\ell_2}(\mathbf{r}'_2)\\ &+s_{mk_2}(\mathbf{r}_1)s_{mk_1}(\mathbf{r}_2)s^*_{m\ell_2}(\mathbf{r}'_1)s^*_{m\ell_1}(\mathbf{r}'_2)\\ &+s_{m\ell_1}(\mathbf{r}_1)s_{m\ell_2}(\mathbf{r}_2)s^*_{mk_1}(\mathbf{r}'_1)s^*_{mk_2}(\mathbf{r}'_2)\\ &+s_{m\ell_2}(\mathbf{r}_1)s_{m\ell_1}(\mathbf{r}_2)s^*_{mk_2}(\mathbf{r}'_1)s^*_{mk_1}(\mathbf{r}'_2)\Big]\end{aligned} \tag{17}$$

and

$$\begin{aligned}\vartheta^{B,m}_{k_1k_2\ell_1\ell_2}(\mathbf{r}_1,\mathbf{r}_2|\mathbf{r}'_1,\mathbf{r}'_2)=\frac{i}{2}\Big[&s_{mk_1}(\mathbf{r}_1)s_{mk_2}(\mathbf{r}_2)s^*_{m\ell_1}(\mathbf{r}'_1)s^*_{m\ell_2}(\mathbf{r}'_2)\\ &+s_{mk_2}(\mathbf{r}_1)s_{mk_1}(\mathbf{r}_2)s^*_{m\ell_2}(\mathbf{r}'_1)s^*_{m\ell_1}(\mathbf{r}'_2)\\ &-s_{m\ell_1}(\mathbf{r}_1)s_{m\ell_2}(\mathbf{r}_2)s^*_{mk_1}(\mathbf{r}'_1)s^*_{mk_2}(\mathbf{r}'_2)\\ &-s_{m\ell_2}(\mathbf{r}_1)s_{m\ell_1}(\mathbf{r}_2)s^*_{mk_2}(\mathbf{r}'_1)s^*_{mk_1}(\mathbf{r}'_2)\Big]\end{aligned} \tag{18}$$

are suitable to expand any density matrix γ_2^s. Functions $\vartheta^{A,B,m}$ meet all the necessary symmetry properties of γ_2^s [22], and the expansion coefficients have the following symmetries

$$\begin{aligned} g^{A,m}_{k_1k_2\ell_1\ell_2} &= g^{A,m}_{k_2k_1\ell_2\ell_1} = g^{A,m}_{\ell_1\ell_2k_1k_2},\\ g^{B,m}_{k_1k_2\ell_1\ell_2} &= g^{B,m}_{k_2k_1\ell_2\ell_1} = -g^{B,m}_{\ell_1\ell_2k_1k_2}.\end{aligned} \tag{19}$$

This representation offers a natural and easy way to reproduce the required electron–electron cusp condition [16, 23] for the two-particle density matrix. In one dimension, for near index pairs ℓ_1, ℓ_2 and k_1, k_2 the expansion coefficients should satisfy [24]

$$g^{A,B,m}_{\ell_1\ell_2k_1k_2}\approx\left(1+\tfrac{1}{2}(|\ell_1-\ell_2|+|k_1-k_2|)\cdot 2^{-m}\right)g^{A,B,m}_{LLKK}. \tag{20}$$

Here, $L=\lfloor(\ell_1+\ell_2+1)/2\rfloor$ and $K=\lfloor(k_1+k_2+1)/2\rfloor$, with $\lfloor x\rfloor$ meaning the floor of x.

Tracing one of the space variables, the one-particle spin-traced density matrix can be written as

$$\gamma_1^{s[m]}(\mathbf{r}|\mathbf{r}')=\sum_{k,\ell}\Big[g^{A,m}_{k\ell}\vartheta^{A,m}_{k\ell}(\mathbf{r}|\mathbf{r}')+g^{B,m}_{k\ell}\vartheta^{B,m}_{k\ell}(\mathbf{r}|\mathbf{r}')\Big], \tag{21}$$

where the expanding functions are

$$\vartheta^{A,m}_{k\ell}(\mathbf{r}|\mathbf{r}')=\frac{1}{2}\left[s_{mk}(\mathbf{r})s^*_{m\ell}(\mathbf{r}')+s_{m\ell}(\mathbf{r})s^*_{mk}(\mathbf{r}')\right], \tag{22}$$

and

$$\vartheta^{B,m}_{k\ell}(\mathbf{r}|\mathbf{r}')=\frac{i}{2}\left[s_{mk}(\mathbf{r})s^*_{m\ell}(\mathbf{r}')-s_{m\ell}(\mathbf{r})s^*_{mk}(\mathbf{r}')\right]. \tag{23}$$

Their symmetry properties are similar to those of the two-electron density matrix basis functions.

The mth level approximation of the electron density arises by taking the diagonal element of (21)

$$\varrho^{[m]}(r) = \sum_{k,\ell}\left(g^{A,m}_{k\ell}\vartheta^{A,m}_{k\ell}(\mathbf{r}|\mathbf{r}) + g^{B,m}_{k\ell}\vartheta^{B,m}_{k\ell}(\mathbf{r}|\mathbf{r})\right). \tag{24}$$

In the case, if the scaling functions are real, which is rather common, $\vartheta^{B,m}_{k\ell}(\mathbf{r}|\,\mathbf{r}) = 0$, which leads to

$$\varrho^{[m]}(\mathbf{r}) = \sum_{k\ell} g^{A,m}_{k\ell} s_{mk}(\mathbf{r}) s_{m\ell}(\mathbf{r}). \tag{25}$$

It is important to notice, that if the supports of the scaling functions do not overlap, i.e., the product $s_{mk}(\mathbf{r})$ $s_{m\ell}(\mathbf{r})$ will be zero, the coefficient $g^{A,m}_{k\ell}$ does not count in the expansion of the density, nor to that of the kinetic or external potential energy functionals, thus it can be chosen arbitrarily.

It should also be noted, that the products s_{mk} $(\mathbf{r})$ $s_{m\ell}(\mathbf{r})$ do not constitute a basis of the density in the following sense. It may be possible, that more mth level expansions, with different sets of coefficients $g^{A,m}_{k\ell}$ exist for one given density, i.e. expansion (25) is not unique.

Based on some general physical properties we have suggested a Weizsäcker-type expression

$$g^{A,m}_{k\ell} = 2^{-m/2}\sqrt{\varrho}(2^{-m}(k+\eta))\sqrt{\varrho}(2^{-m}(\ell+\eta)) \tag{26}$$

as a first approximation of the expansion coefficients [25]. We have also shown that taking into account the proper antisymmetry property of the wave function leads to a further refinement of the scaling function coefficients (26), moreover, inclusion of electron correlation effects is also possible in a natural way.

5 Expansion of energy terms

Using the density, the spin-traced one- and two-electron density matrices, the kinetic energy T, electron–electron interaction, and external potential energy expectation values can be expressed as

$$\langle\hat{T}\rangle = \frac{1}{2}\int\left(\frac{\mathrm{d}}{\mathrm{d}\mathbf{r}}\frac{\mathrm{d}}{\mathrm{d}\mathbf{r}'}\gamma^s_1(\mathbf{r}|\mathbf{r}')\right)\Bigg|_{\mathbf{r}=\mathbf{r}'}\mathrm{d}\mathbf{r} \tag{27}$$

$$\langle\hat{W}\rangle = \int\frac{\gamma^s_2(\mathbf{r}_1,\mathbf{r}_2|\mathbf{r}_1,\mathbf{r}_2)}{|\mathbf{r}_1-\mathbf{r}_2|}\mathrm{d}\mathbf{r}_1\mathrm{d}\mathbf{r}_2 \tag{28}$$

$$\langle\hat{V}\rangle = \int\varrho(\mathbf{r})v(\mathbf{r})\mathrm{d}\mathbf{r}, \tag{29}$$

where $v(\mathbf{r})$, the external potential is usually a sum of terms in the form $Z_\alpha|\mathbf{r}-\mathbf{R}_\alpha|^{-1}$, where $\mathbf{R}_\alpha$ indicates the site of the αth nucleus with charge Z_α. With expansion (24), (21) and (16) of the density and the density matrices the kinetic (27), the electron–electron interaction (28) and the external potential energy (29) can be written in one dimension by lengthy but straightforward algebraic calculations, applying the dilation and translation properties of the scaling functions as

$$\langle\hat{T}\rangle^{[m]} = \frac{1}{2}\sum_{k\ell} g^{A,m}_{k\ell}\mathcal{T}_m(k-\ell) \tag{30}$$

$$\langle\hat{W}\rangle^{[m]} = \sum_{k_1k_2\ell_1\ell_2} g^{A,m}_{k_1k_2\ell_1\ell_2}\times\mathcal{W}_m(k_1-\ell_1,k_2-\ell_2,k_1-k_2) \tag{31}$$

$$\langle\hat{V}\rangle^{[m]} = \sum_\alpha Z_\alpha\sum_{k\ell} g^{A,m}_{k\ell}\times\mathcal{V}_m(2^{-m}k-R_\alpha,2^{-m}\ell-R_\alpha) \tag{32}$$

with the expansion coefficients $g^{A,m}_{k\ell}$ and $g^{A,m}_{k_1k_2\ell_1\ell_2}$ of the one and two-electron density matrix. R_α are expressed in units of the grid distance b.

Using the refinement equation (8), the functions covered by the calygraphical letters can be originated from integrals

$$\mathcal{T}_0(k) = \int s'_{00}(x)s'^*_{0k}(x)\mathrm{d}x, \tag{33}$$

$$\mathcal{W}_0(k,\ell,j) = \int\frac{s_{00}(x_1)s_{00}(x_2)s^*_{0k}(x_2)s^*_{0\ell}(x_1)}{|x_1-x_2-j|}\mathrm{d}x_1\mathrm{d}x_2, \tag{34}$$

$$\mathcal{V}_0(q_k,q_\ell) = \int\frac{s_{00}(x-q_k)s^*_{00}(x-q_\ell)}{|x|}\mathrm{d}x, \tag{35}$$

where $s'(x) = \mathrm{d}s(x)/\mathrm{d}x$. For higher resolution levels m, the values can be derived from (33)–(35) by a simple scaling transformation as $\mathcal{T}_m = 2^m\mathcal{T}_0$, $\mathcal{W}_m = 2^{2m}\mathcal{W}_0$ and $\mathcal{V}_m = 2^m\mathcal{V}_0$, respectively.

According to these results energy functionals can be expanded by three types of universal functions. Due to the compact support of scaling functions the overlap in expressions (33)–(35) is zero for most values of the arguments. Function $\mathcal{T}$ is defined for one integer variable, making it especially simple to manage, as it represents a series of few numbers for the arguments $|k| < N_s$. Similarly, $\mathcal{W}$ is to be calculated on an integer grid of three variables with the constraint $|k|, |\ell| < N_s$. The numerical storage of its values is much easier than the similar problem of storing two-electron integrals in usual numerical approaches. Moreover, since they do not depend on the actual system properties, only on the type of wavelets, the values of $\mathcal{T}$ and $\mathcal{W}$ can be calculated and stored in advance. The universal function $\mathcal{V}$ is significant for the real values $|q_1 - q_2| < N_s$ and zero outside of this range.

According to the above considerations the compact support of the basis functions and the functional forms of the matrix elements (33)–(35) indicate that only the immediate neighborhood of the basis functions contribute

to the Hamiltonian matrix elements, causing that the sparse matrix H contains $O(N)$ number of non-zero elements. There are known methods for $O(N)$ diagonalization of sparse matrices. Moreover, in the next section we will show, that it is possible to replace the fine resolution parts (nuclear cusps) of the wave function by pre-determined fixed building blocks. All these advantageous properties offer the possibility of a calculation method of $O(N)$.

6 MRA representations of the nuclear and electron–electron cusps in the He atom

One of the most favorable properties of MRA expansions is the relatively easy handling of sharp peaks and changes in the represented distributions. Since Kato's original work [16], it is well known, that the wave function as well as the density and the two-particle density operator [23] are continuous at the singular points of the Hamiltonian operator, however their derivatives show discontinuity. These questions have recently been studied [26] in relation with the complexity of the wave function.

With the following study we illustrate that realistic electronic systems are adequately described by wavelet expansions at moderately fine resolution levels with a manageable number of basis function, despite of the singularities appearing due to the Coulomb interactions. The simplest system which shows both the nuclear and the electron-electron cusp is the helium atom described by a correlated wave function. We will use it as a reference, as many previous studies (see e.g., [27–30]) provide a precise description of the wave function. Moreover, it offers the possibility to test the three dimensional behavior of the MRA expansion and the necessary level of resolution around the cusps.

For two electrons in a singlet state the antisymmetric wave function is a product of the symmetric spatial part $\Psi(\mathbf{r}_1, \mathbf{r}_2)$ and the antisymmetric spin function. As the two-particle density operator carries essentially the same information as the wave function for two electrons, we will study $\Psi(\mathbf{r}_1, \mathbf{r}_2)$ instead of γ_2^s in the following considerations. The z axis of the system of reference is chosen along the vector $\mathbf{r}_1$ and the xz plane is determined by the plane of the $\mathbf{r}_1$ and $\mathbf{r}_2$ vectors. With this choice, the component form of the electron coordinates is $\mathbf{r}_1 = (0, 0, z_1)$ and $\mathbf{r}_2 = (x_2, 0, z_2)$.

The 3D scaling function representation of the wave function at resolution level m is given by the expression

$$\Psi^{[m]}(\mathbf{r}_1, \mathbf{r}_2) = \sum_{i_1 j_1 k_1} \sum_{i_2 j_2 k_2} c^m_{i_1 j_1 k_1, i_2 j_2 k_2} s_{mi_1}(x_1) s_{mj_1}(y_1) s_{mk_1}(z_1) \times s_{mi_2}(x_2) s_{mj_2}(y_2) s_{mk_2}(z_2). \quad (36)$$

For simplicity, we have given a non-symmetric representation, instead of the form similar to (16). In the chosen system of reference

$$\Psi^{[m]}(0, 0, z_1; x_2, 0, z_2) = \sum_{k_1 i_2 k_2} d^m_{k_1 i_2 k_2} s_{mk_1}(z_1) s_{mi_2}(x_2) s_{mk_2}(z_2), \quad (37)$$

where

$$d^m_{k_1 i_2 k_2} = \sum_{i_1 j_1 j_2} c^m_{i_1 j_1 k_1, i_2 j_2 k_2} s_{mi_1}(0) s_{mj_1}(0) s_{mj_2}(0). \quad (38)$$

In Fig. 1, we present the $m = 3$ level expansion of the wave function (37) for $x_2 = 0$ using Daubechies basis set with $N_s = 4$. The reference wave function is taken from reference [31]. The nuclear cusp is clearly identified at the positions $z_1 = z_2 = 0$ (both electrons are at the nucleus), and the expected closely exponential form is also well reproduced. We can realize, that the plot shows a rather smooth surface even at relatively low resolution level, except the immediate neighborhood of the cusp positions, where the internal structure of the scaling functions can be observed. The edges along the lines $z_1 = 0$ or $z_2 = 0$ correspond to those nuclear cusps, when only one of the electron positions coincides with the nucleus.

The electron-electron cusp is expected where the two electrons are at the same position, i.e., $z_1 = z_2$. By a careful investigation of the figure, we can realize a slight valley in the front side of the peak along the diagonal line $z_1 = z_2$. In order to better visualize the effect, we have plotted an orthogonal cross-section of the surface in Fig. 2. Although with a moderate oscillation, the MRA expansion sufficiently reproduces the electron-electron cusp describing the electron correlation.

Finally, we have studied the extension of the spatial regions where at a given resolution level m the

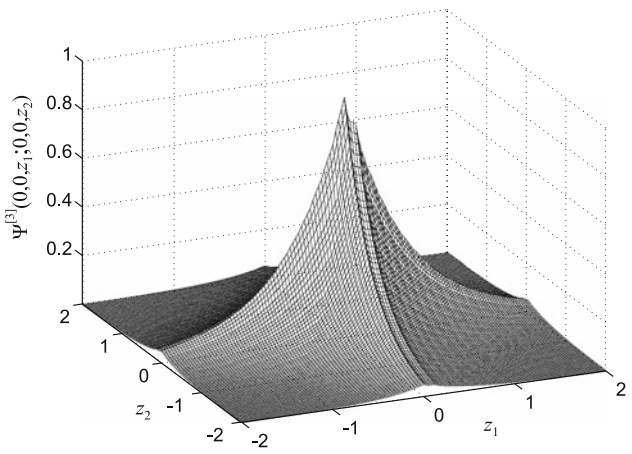

Fig. 1 Level $m = 3$ scaling function expansion of the He wave function $\Psi(\mathbf{r}_1, \mathbf{r}_2)$ in arbitrary units (Ψ is not normalized). For the coordinates z_1 and z_2 atomic units were used

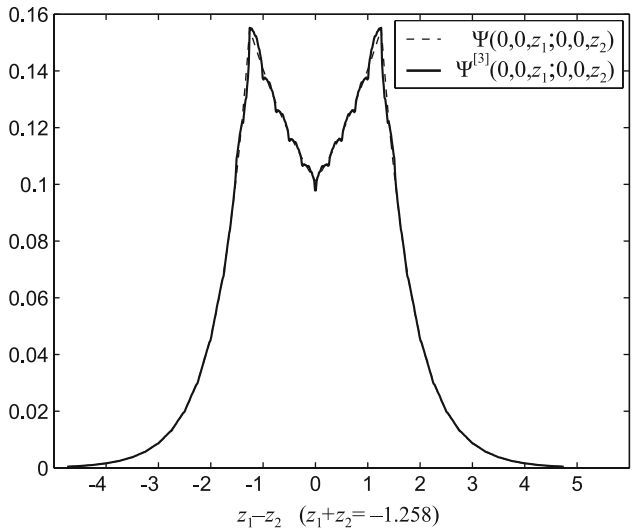

Fig. 2 Cross-section of the surface $\Psi(0, 0, z_1; 0, 0, z_2)$ in a perpendicular direction to the diagonal $z_1 = z_2$. The electron-electron cusp manifests itself as a V-shaped folding in the curve. The left and right peaks are nuclear cusps at $z_1 = -1.258$, $z_2 = 0$ and $z_1 = 0$, $z_2 = -1.258$, respectively. Both the numerical wave function Ψ of Ref. [31] and its $m = 3$ level scaling function expansion $\Psi^{[3]}$ are shown in arbitrary units. For the difference coordinate $z_1 - z_2$ atomic units were used

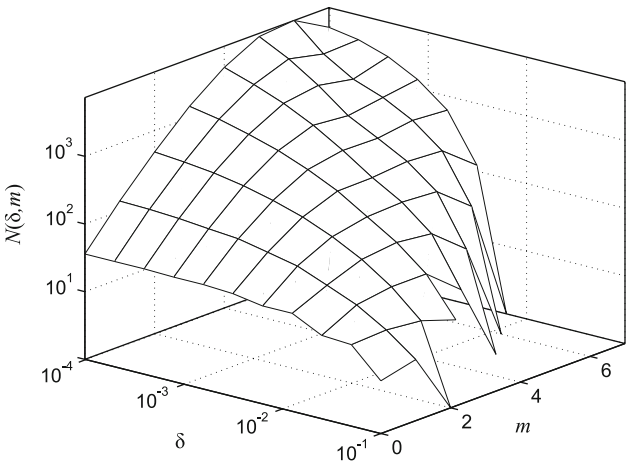

Fig. 3 The number of configuration space cells $N(\delta, m)$ where further refinement is necessary in the $(0, 0, z_1; 0, 0, z_2)$ plane of the He wave function's mth level expansion as a function of the refinement level m and the error criterion δ on a logarithmic scale. If refinement is not necessary (i.e., $N(\delta, m) = 0$), no point is plotted

approximation $\Psi^{[m]}$ is not satisfactory. In order to quantitatively characterize the size of the above domain, let us consider that the scaling function expansion (36) naturally divides the configuration space to non-overlapping multidimensional cubic cells of edge length 2^{-m}. The Kth such cell will be denoted by $\mathcal{D}_K^{[m]}$. Normalizing the wave function by its global maximum value, we count the number of cells where the deviation of the wave functions exceeds a critical value δ

$$N(\delta, m) = \text{number of } K \text{ indices where } \max_{(\mathbf{r}_1,\mathbf{r}_2)\in\mathcal{D}_K^{[m]}} |\Psi(\mathbf{r}_1,\mathbf{r}_2) - \Psi^{[m]}(\mathbf{r}_1,\mathbf{r}_2)| > \delta. \quad (39)$$

In Fig. 3, we have plotted $N(\delta, m)$ as a function of the precision requirement δ and the resolution level m. We can conclude, that at high precision approximations (δ is small) the number of cells where a further refinement of the wave function is necessary increases almost exponentially. At intermediate precision requirements $N(\delta, m)$ saturates for a moderate m, whereas for larger δ we can realize, that the higher resolution levels become quickly unimportant. As a general rule, we expect that at a given precision level the number of regions for further refinement initially increases exponentially, and after attaining a maximum it drops to zero. The initial exponential growth at rough resolutions can be explained by the fact, that the precision constraint demands a full space refinement. On the other hand, as we have shown [22], both the extremely rough and the very fine resolution level wavelet contributions should necessarily disappear, causing $N(\delta, m) \to 0$ if $m \to \infty$. Fig. 3 shows, that depending on the precision requirement $N(\delta, m) = 0$ for relatively small m already.

Considering that the linear cell size decreases as $\sim 2^{-m}$, the total spatial extension of insufficient approximations decreases monotonically with the resolution level.

These facts involve that a deliberate omission of fine details in solving the Schrödinger equation leads to appropriate physical results. Moreover, it is clear from the above considerations, that the really fine resolution structure of the molecules is originated solely from the cusps, which, on the other side, show a universal structure due to Kato's theorem. As a future prospect and a further simplification of the calculations we suggest that the universal fine structure of the molecules (cusps) is replaced by predefined building blocks (high resolution level wavelet expansion parts) and the numerical solution of the eigenvalue problem is performed only up to the medium resolution parts.

7 Avoiding the unfavorable algorithmic complexity in terms of the refinement level

Any element of the Hilbert space $\Psi \in L^2(\mathbb{R})$ can be exactly decomposed into orthogonal components by multiresolution analysis as

$$\Psi(x) = \sum_{\ell\in\mathbb{Z}} c_\ell \, s_{0\ell}(x) + \sum_{m=0}^{\infty}\sum_{\ell\in\mathbb{Z}} d_{m\ell} \, w_{m\ell}(x). \quad (40)$$

If $\Psi(x)$ is a compactly supported or a fast decaying function, one can realize, that the total number of expansion coefficients in a given resolution level m scales as $\sim 2^m$ (or

in D dimensions $\sim 2^{mD}$), which makes the above expansion unapplicable for practical calculations. The exponential increase of the number of necessary basis functions can be avoided by an adaptive refinement strategy, including wavelets only in those regions of the molecules, where the details of the electron structure require it. This idea is explained in the following.

The resolution structure of the wave function can be characterized by the series of projections

$$\begin{aligned} P_0\Psi &= \sum_{\ell\in\mathbb{Z}} c_\ell\, s_{0\ell}, \\ Q_0\Psi &= \sum_{\ell\in\mathbb{Z}} d_{0\ell}\, w_{0\ell}, \\ Q_1\Psi &= \sum_{\ell\in\mathbb{Z}} d_{1\ell}\, w_{1\ell}, \\ &\cdots \end{aligned} \tag{41}$$

P_0, Q_0, Q_1, etc. are the orthogonal projection operators to subspaces V_0, W_0 W_1, etc. The wave function Ψ projected to subspace V_M is

$$\Psi^{[M]} = P_0\Psi + \sum_{m=0}^{M-1} Q_m\Psi. \tag{42}$$

For characterizing the importance of a given resolution level W_m, a measure for the level complexity can be introduced as $\Omega_m = \|Q_m\Psi\|^2$. The detail spaces W_m with negligible Ω_m can be completely ignored.

Often, even if

$$\Omega_m = \|Q_m\Psi\|^2 = \sum_{\ell\in\mathbb{Z}} d_{m\ell}^2 \tag{43}$$

is rather large, the significant part of the sum arises from a very restricted space domain [15, 32]. Using the restricted detail space $\widetilde{W}_m = \text{span}\{w_{m\ell}|$ where $d_{m\ell}$ is significant$\}$ can help to keep the computation demands lower, provided a method for guessing the magnitude of the coefficients $d_{m\ell}$ *before having them already calculated* can be given. A *predictive* method is needed using only the results of the already calculated $(m-1)$th, $(m-2)$th, etc. levels. The in-level truncation of the Hilbert space is symbolized here by a tilde mark above the quantity's sign, i.e.,

$$\tilde{\Psi}^{[M]} = P_0\Psi + \sum_{m=0}^{M-1} \tilde{Q}_m\Psi, \tag{44}$$

with $\tilde{Q}_m$ being the projector to the in-level truncated subspace $\widetilde{W}_m$.

According to case studies of exactly solvable model systems [33], high resolution wavelets with exponentially small Ω_m are negligible. At lower m values only a fractional part of them have essential contribution in the expansion, mostly localized to quickly changing parts of the exact wave functions caused by the singularities of the external potential. It has turned out [34], that high necessary expansion levels are also induced by the careless treatment of the kinetic energy operator. A further study of similar questions can be found in [35]. In the following discussion we will concentrate on avoiding high required resolution caused both by the kinetic energy operator and by singular regions of the external potential.

Clearly, a method is necessary for giving the essential coefficients in (40), *prior to calculating the complete resolution level*. Let us suppose, that the Mth level approximation of the wave function Ψ

$$\widetilde{\Psi}^{[M]}(x) = \sum_{\ell\in\widetilde{V}_0} \tilde{c}_\ell^{[M]}\, s_{0\ell}(x) + \sum_{m=0}^{M-1}\sum_{\ell\in\widetilde{W}_m} \tilde{d}_{m\ell}^{[M]}\, w_{m\ell}(x). \tag{45}$$

is known. The shorthand notation $\ell \in \widetilde{W}_m$, indicates, that the summation index ℓ is restricted to the wavelets $w_{m\ell}$ belonging to the in-level truncated subspace $\widetilde{W}_m$. Based on this knowledge, the $(M+1)$th level coefficients can be predicted in the following way.

Tymczak and Wang [36] suggested a "bootstrap" algorithm for selecting the most important $(M+1)$th level coefficients, based on the approximate scaling behavior of $\tilde{d}_{m\ell}^{[M]}$. This mathematical argument implies that at the extension step of the Hilbert space to $\widetilde{\mathcal{H}}^{[M+1]} = \widetilde{\mathcal{H}}^{[M]} \oplus \widetilde{W}_M$ the subspace $\widetilde{W}_M$ should contain only those wavelets $w_{M\ell}$ which belong to those spatial domains that have been considered important in the previous Mth resolution level. The number of extension wavelets $w_{M\ell}$ introduced by the bootstrap algorithm is, however, much larger than it is necessary for the appropriate description of the wave function, as we have found it in [15] and pointed out also at the end of the previous Section.

Although the unnecessary wavelets are singled out later, after solving the Schrödinger equation in $\widetilde{\mathcal{H}}^{[M+1]}$ and dropping the small coefficients $\tilde{d}_{M\ell}^{[M+1]}$, this approach is clearly not optimal. An essential improvement can be achieved by an a priori selection of the really important coefficients based on a physical selection criterion. This procedure is based on the ideas published in [32] and [37].

The quality of the Mth level approximation of the eigenvalues and eigenvectors can be characterized by the error function

$$\widetilde{\Delta}^{[M]} = (H - \widetilde{E}^{[M]})\widetilde{\Psi}^{[M]} \neq 0. \tag{46}$$

As $\widetilde{\Psi}^{[M]}$ is the solution of the Schrödinger equation in the restricted Hilbert space $\widetilde{\mathcal{H}}^{[M]}$, the error function (46) is orthogonal to it, i.e. $\langle w_{m\ell}|(H - \widetilde{E}^{[M]})|\widetilde{\Psi}^{[M]}\rangle = 0$ if $w_{m\ell} \in \widetilde{\mathcal{H}}^{[M]}$. On the other hand, one expects that the wavelet extensions are essential in those spatial domains where the error function is large. The contribution of the wavelet $w_{M\ell} \in W_M$ to $\widetilde{\Delta}^{[M]}$ is measured by

$$r_{M\ell} = \left|\langle w_{M\ell}|\widetilde{\Delta}^{[M]}\rangle\right|^2 = \left|\langle w_{M\ell}|H - \widetilde{E}^{[M]}|\widetilde{\Psi}^{[M]}\rangle\right|^2. \quad (47)$$

If $r_{M\ell}$ is large enough, the wavelet $w_{M\ell}$ should be included in the further calculations, if not, it can be omitted.

Combining the bootstrap algorithm with the physical selection criterion (47) determines the in-level truncated extension detail space $\widetilde{W}_M$. In fact, we have sorted the $r_{M\ell}$ to descending order and we have dropped all wavelets with the smallest $r_{M\ell}$, until the cumulated value $\sum_\ell r_{M\ell}$ did not exceed a preselected precision criterion η. The Schrödinger equation is solved with this in the truncated Hilbert space $\widetilde{\mathcal{H}}^{[M+1]} = \widetilde{\mathcal{H}}^{[M]} \oplus \widetilde{W}_M$. This method is adaptive in the sense, that due to the physical measure (47) the selection is adapted both to the nature of the described system through the external potential in H and to the numerical inaccuracies in the wavelet representation of the kinetic energy operator.

The gain by this adaptive method concerning the number of necessary wavelets compared to wavelet-based calculations with no further considerations is rather large. The improvement relative to the simple bootstrap algorithm is also considerable, as controlling the criterion (47) scales linearly with the number of tested wavelets, whereas the solution of the eigenvalue problem in this larger subspace involved in the bootstrap procedure has a much unfavorable algorithmic behavior.

As an example, we consider the simple harmonic oscillator, which is a good model for vibrations of strong bonds, e.g., the C–F stretching mode. In the ground state calculation the ordinary solution includes $\dim W_6 = 646$ basis functions, whereas for the adaptive one $\dim \widetilde{W}_6 = 296$, both using the error condition $\eta = 10^{-9}$. Adaptive calculations have been carried out for harmonic oscillators and the resulting projected wave functions are compared in Tables 1 and 2. The difference of the norms of the mth resolution expansion coefficients of $\Psi^{[M]}$ of the level truncated method and those of the in-level truncated method $\widetilde{\Psi}^{[M]}$ is shown in the tables for moderate and strict error requirements. The wave function $\widetilde{\Psi}^{[M]}$ calculated in the in-level truncated Hilbert space is expected to significantly deviate from the eigenstate $\Psi^{[M]}$ received without truncation if the required precision is low. On the other hand, for high precision (small η) $\widetilde{\Psi}^{[M]}$ approximates $\Psi^{[M]}$ very well.

Tables 1 and 2 contain the deviations $\delta\|P_0\widetilde{\Psi}_0^{[M]}\|^2 = \|P_0\widetilde{\Psi}_0^{[M]}\|^2 - \|P_0\Psi_0^{[M]}\|^2$ and $\delta\|Q_m\widetilde{\Psi}_0^{[M]}\|^2 = \|Q_m\widetilde{\Psi}_0^{[M]}\|^2 - \|Q_m\Psi_0^{[M]}\|^2$ for precisions $\eta = 10^{-4}$ and $\eta = 10^{-8}$, respectively. In the intermediate precision case the error of the wave function saturates with increasing resolution level M. As a consequence, an excessive refinement of the wave function is ineffective. In the high precision case the wave function $\widetilde{\Psi}^{[M]}$, obtained using the adaptive fine structure localization method, results in an excellent approximation to $\Psi^{[M]}$. The error introduced by the in-level truncation is less, than that of the level-truncation, up to the resolution level $M = 4$. At level $M = 5$ the in-level truncation error is below the computer's arithmetic precision.

Similarly to the wave function the energy saturates with increasing resolution at low precisions [33]. These facts

Table 1 The deviation of the in-level truncated wave function $\widetilde{\Psi}_0^{[M]}$ from that of $\Psi_0^{[M]}$ due to fine structure localization with $\eta = 10^{-4}$ in the detail spaces V_0, W_0, ..., W_4

M	$\delta\|P_0\widetilde{\Psi}_0^{[M]}\|^2$	$\delta\|Q_0\widetilde{\Psi}_0^{[M]}\|^2$	$\delta\|Q_1\widetilde{\Psi}_0^{[M]}\|^2$	$\delta\|Q_2\widetilde{\Psi}_0^{[M]}\|^2$	$\delta\|Q_3\widetilde{\Psi}_0^{[M]}\|^2$	$\delta\|Q_4\widetilde{\Psi}_0^{[M]}\|^2$
1	0.00359×10^{-7}	-0.00359×10^{-7}				
2	-0.57935×10^{-7}	0.57900×10^{-7}	0.00341×10^{-8}			
3	-1.33904×10^{-7}	1.15127×10^{-7}	1.87090×10^{-8}	0.6884×10^{-10}		
4	-1.11325×10^{-7}	1.01237×10^{-7}	1.19756×10^{-8}	0.3925×10^{-10}	0.429×10^{-11}	
5	-1.11955×10^{-7}	0.99627×10^{-7}	1.26402×10^{-8}	-2.9725×10^{-10}	1.460×10^{-11}	8×10^{-14}

Table 2 The deviation of the in-level truncated wave function $\widetilde{\Psi}_0^{[M]}$ from that of $\Psi_0^{[M]}$ due to fine structure localization with $\eta = 10^{-8}$ in the detail spaces V_0, W_0, …, W_3

M	$\delta\|P_0\widetilde{\Psi}_0^{[M]}\|^2$	$\delta\|Q_0\widetilde{\Psi}_0^{[M]}\|^2$	$\delta\|Q_1\widetilde{\Psi}_0^{[M]}\|^2$	$\delta\|Q_2\widetilde{\Psi}_0^{[M]}\|^2$	$\delta\|Q_3\widetilde{\Psi}_0^{[M]}\|^2$
1	0.205×10^{-11}	-0.205×10^{-11}			
2	0.023×10^{-11}	-0.023×10^{-11}			
3	-5.933×10^{-11}	5.902×10^{-11}	3.2×10^{-13}		
4	-5.408×10^{-11}	5.457×10^{-11}	-5.1×10^{-13}	2×10^{-14}	
5	-3.550×10^{-11}	3.530×10^{-11}	1.8×10^{-13}	3×10^{-14}	-10^{-14}

The error in the detail spaces W_4, W_5,… is less than the numerical precision of the computer arithmetics

emphasize the importance of choosing matching values for the precision requirement η and the granularity level M.

8 Conclusions

We have outlined how it is possible to formulate the quantum mechanical eigenstate problem, as well as the representation of the wave function, density matrices in terms of the wavelet or multiresolution analysis. The main idea is an initially rough description of the system, including only details in large scale. Consecutively adding finer resolution details is possible by adding wavelets to the orthonormal basis set, which describe short range changes in the wave function. It turned out, that the contribution of such fine details exponentially disappears as the level of resolution M increases. This fact offers the possibility of truncating the applied basis set to a sometimes surprisingly rough description level, at the same time approximating the wave function with a sufficient precision.

We have found the same experience by describing the nuclear and electron-electron cusp properties of the correlated spatial wave function $\Psi(\mathbf{r}_1, \mathbf{r}_2)$ of the He atom in three dimensions. Already the $M = 3$ level expansion leads to a quite acceptable reproduction of the singularities of Ψ around the nuclear and two-particle cusps.

Still, even for moderate values of M, the number of basis functions of approximate wavelet expansions increases as $\sim 2^{DM}$, making practical numerical calculations impossible. In this contribution we have suggested an adaptive method, by which it is possible to exclude a large number of fine resolution basis functions, based on a prediction of their negligible contribution to the wave function. Testing the predictive algorithm on a model system we have found, that the number of significant basis functions is considerably less than the dimension of the detail subspaces included in full calculations.

The main benefit from using the highly uniform basis set of scaling functions and wavelets which are generated by simple scaling and displacement transformations of mother functions is the extremely compact structure of the one- and two-electron integral list. In fact, only a few numbers have to be calculated and stored in advance, depending only on the chosen mother function, and are completely independent of the studied system.

Acknowledgments This work was supported by the Bolyai János Research Foundation and the National Office of Research and Technology (NKTH, Hungary) Grant No. MX-16/2007.

References

1. Christopoulos C, Skodras A, Ebrahimi T (2000) IEEE Trans Consumer Electron 46:1103
2. MJ2 Format Standard. ISO/IEC 15444-3:2002/Amd 2:2003
3. Martucci SA, Sodagar I, Chiang T, Zhang Y-Q (1997) IEEE Trans Circuits Syst Video Technol 7:109–118
4. Chai B-B, Vass J, Zhuang X (1999) IEEE Trans Image Proc 8:774–784
5. Goedecker S, Ivanov OV (1998) Solid State Commun 105:665
6. Cho K, Arias TA, Johannopoulos JD, Lam PK (1993) Phys Rev Lett 71:1808
7. Wei S, Chou MY (1996) Phys Rev Lett 76:2650
8. Arias TA (1999) Rev Mod Phys 71:267
9. Engenes TD, Arias TA (2002) Phys Rev B 65:165106
10. Flad H-J, Hackbusch W, Luo H, Kolb D (2005) J Comput Phys 205:540–566
11. Yanai T, Fann GI, Gan Z, Harrison RJ, Beylkin G (2004) J Chem Phys 121:6680
12. Harrison RJ, Fann GI, Yanai T, Gan Z, Beylkin G (2004) J Chem Phys 121:11587
13. Johnson BR, Mackey JL, Kinsey JL (2001) J Comput Phys 168:356
14. Maloney A, Kinsey JL, Johnson BR (2002) J Chem Phys 117:3548
15. Pipek J, Nagy S (2005) J Chem Phys 123:144107
16. Kato T (1957) Pure Appl Math 10:151
17. Chui CK (1992) An introduction to wavelets. Academic Press, San Diego
18. Daubechies I (1992) Ten lectures on wavelets. In: CBMS-NSF regional conference series in applied mathematics, vol 61. SIAM, Philadelphia
19. Dahmen W, Micchelli CA (1993) SIAM J Numer Anal 30:507
20. Genovese L, Neelov A, Goedecker S, Deutsch T, Ghasemi SA, Willand A, Caliste D, Zilberberg O, Rayson M, Bergman A, Schneider R (2008) J Chem Phys 129:014109
21. Flad H-J, Hackbusch W, Kolb D, Schneider R (2002) J Chem Phys 116:9641
22. Nagy S, Pipek J (2001) Int J Quantum Chem 84:523
23. Bingel W (1966) Theor Chim Acta 5:341
24. Pipek J, Nagy S (2001) Phys Rev A 64:052506
25. Pipek J, Nagy S (2003) J Chem Phys 119:8257
26. Yserentant H (2007) Regularity properties of wavefunctions and the complexity of the quantum-mechanical N-body problem (unpublished)
27. Roothaan CCJ, Weiss AW (1960) Rev Mod Phys 32:194
28. Power JD, Somorjai RL (1972) Phys Rev A 5:2401
29. Thakkar AJ, Smith VH Jr (1977) Phys Rev A 15:1
30. Drake GWF, Cassar MM, Nistor RA (2002) Phys Rev A 65:054501
31. Green LC, Lewis MN, Mulder MM, Wyeth CW, Woll JW Jr (1954) Phys Rev 93:273
32. Dahmen W (2001) J Comput Appl Math 128:123
33. Pipek J, Nagy S (2006) J Chem Phys 125:174107
34. Pipek J, Nagy S (2009) J Math Chem 46:261–282
35. Pipek J, Nagy S (2008) Chem Phys Lett 464:103
36. Tymczak CJ, Xiao-Qian Wang (1997) Phys Rev Lett 78:3654
37. Ladányi K, Lévay P, Apagyi B (1988) Phys Rev A 38:3365